ORIGINAL ARTICLE

Comparison of the anti-cancer activity of 5-aminolevulinic acid-mediated photodynamic therapy after continuous wave and pulse irradiation in different histological types of canine mammary sarcoma tumors

Ozge Turna[1] · Asuman Deveci Ozkan[2] · Gamze Guney Eskiler[2] · Aslihan Baykal[1] · Ozge Ozten[3] · Funda Yildirim[4] · Elif Ilkay Armutak[5] · Ali Furkan Kamanli[6] · Hyun Soo Lim[6] · Suleyman Kaleli[2] · Guven Kasikci[1] · Salih Zeki Yildiz[7]

Abstract

Canine mammary sarcoma tumors (CMST) are the most aggressive tumors with poor prognosis in dogs. Due to inadequate treatment options for CMST, recent studies have focused on alternative treatment strategies. We previously determined the optimized protocol of 5-ALA-based photodynamic therapy (PDT) in canine liposarcoma. However, its molecular mechanisms in the treatment of different histological types of CMST remain unclear.

In this context, we, for the first time, assessed 5-aminolevulinic acid (5-ALA)-PDT–mediated anti-cancer activity and its molecular mechanism after continuous wave (CW) and pulse radiation (PR) on three different histological types (liposarcoma, chondrosarcoma, and osteosarcoma) of CMST cells by WST-1, Annexin V, ROS, acridine orange/propidium iodide staining, RT-PCR, and western blot analysis.

Our findings showed that 5-ALA/PDT significantly suppressed the proliferation of CMST cells ($p < 0.01$) and induced apoptosis via increased ROS level and overexpression of Caspase-9 and Caspase-3 mRNA and cleaved protein levels in especially liposarcoma and chondrosarcoma cells following CW and PR irradiation at 9 J/cm^2. However, the response of CMST cells to 5-ALA was different upon CW and PR irradiation due to differences in their origin.

Collectively, our findings provided the first evidence that 5-ALA-based PDT could be used as an alternative treatment strategy, especially liposarcoma and chondrosarcoma. However, further in vitro and in vivo studies are required to elucidate the underlying molecular mechanism of the efficacy of 5-ALA in CMST cells at the molecular level.

Keywords Canine mammary tumors · Photodynamic therapy · 5-Aminolevulinic acid · Apoptosis

✉ Gamze Guney Eskiler
gamzeguney@sakarya.edu.tr

1 Department of Obstetrics and Gynecology, Faculty of Veterinary Medicine, Istanbul University-Cerrahpasa, Istanbul, Turkey

2 Department of Medical Biology, Faculty of Medicine, Sakarya University, Sakarya, Turkey

3 Department of Biomedical Engineering, Institute of Natural Sciences, Sakarya University of Applied Science, Sakarya, Turkey

4 Department of Pathology, Faculty of Veterinary Medicine, Istanbul University-Cerrahpasa, Istanbul, Turkey

5 Department of Histology and Embryology, Faculty of Veterinary Medicine, Istanbul University-Cerrahpasa, Istanbul, Turkey

6 Department of Electric and Electronics Engineering, Faculty of Technology, Sakarya University of Applied Sciences, Sakarya, Turkey

7 Department of Chemistry, Faculty of Science, Sakarya University, Sakarya, Turkey

Introduction

Canine mammary tumors (CMTs) are the most common type among canine tumors, with molecular and clinical similarities of human breast cancers [1, 2]. The histological classification of CMTs has been published by the World Health Organization, including benign and malignant tumors and dysplasia of the mammary glands [3]. Following this classification, Goldschmidt et al. [4] determine a complete and exhaustive classification scheme as seven benign and 23 malignant histologic subtypes.

Although most malignant CMTs are of epithelial origin (carcinomas), some of them exhibit mesenchymal origin (sarcomas). Additionally, certain malignant CMTs may consist of both epithelial and mesenchymal tissue (malignant mixed tumor) [2–4]. Sarcomas (S) comprise < 13% of all malignant CMTs and are histologically classified into osteosarcomas, fibrosarcomas, chondrosarcomas, and liposarcomas. Canine mammary sarcoma tumors (CMST) tend to metastasize mostly through the hematogenous way. This behavior of the CMST leads to the formation of distant metastasis, poor prognosis and short survival time in dogs [2, 5–7].

Surgery is considered a gold standard treatment choice for CMT, except for inoperable metastatic cases and inflammatory carcinomas. Although a wide-margin surgery is performed, adjuvant treatment options are still experimental in veterinary clinical oncology, including chemotherapy, radiotherapy, and anti-angiogenic therapy [2, 5–9] and remain inadequate for the treatment of CMST cases due to poor prognosis. Therefore, alternative treatment strategies are still required for the treatment of CMST.

Photodynamic therapy (PDT) has emerged as a potential new treatment modality for the suppression of recurrence and metastases of different cancer types with minimal side effects. The efficacy of PDT depends on the types and uptake of photosensitizer, a light source with an optimum wavelength and molecular oxygen for the induction of cell death via oxidative damage [10–12]. 5-Aminolevulinic acid (5-ALA), a precursor of the protoporphyrin IX (PpIX), is one of the most promising second-generation photosensitizers for PDT. The activation of 5-ALA is based on the transformation into the PpIX following irradiation and is specifically uptaken by cancer cells due to higher metabolic activity, and thus, PpIX activation leads to cell death through reactive oxygen species (ROS) production [12–14]. The use of 5-ALA-mediated PDT has been approved by FDA in the treatment of actinic keratosis, esophageal dysplasia, extremities, and trunk/neck and the surgical resection of high-grade gliomas. Additionally, the anti-cancer effects of 5-ALA have been evaluated upon irradiation in different types of cancer, including head and neck cancer, bladder tumors, prostate cancer, gastric cancer, Barrett's esophagus, breast cancer, cervix, vulvar, and vaginal intraepithelial neoplasias cutaneous T-cell lymphoma in preclinical and clinical studies [14]. However, there are limited studies evaluating the effectiveness of 5-ALA-based PDT in the treatment of canine tumors [15, 16]. Our previous study identified the most effective 5-ALA/PDT protocol in different histological types of CMT, including liposarcoma, adenocarcinoma, and carcinosarcoma [17]. However, the underlying molecular mechanism behind 5-ALA/PDT in sarcomas, including liposarcoma, remains unclear. In this context, we evaluated the anti-cancer activity of 5-ALA-mediated PDT and its molecular mechanism in three different histological types of sarcoma (S) cells (liposarcoma, osteosarcoma, and chondrosarcoma) after laser irradiation with different modes [continuous wave (CW) and pulse radiation (PR)] by further molecular analysis.

Material and methods

Ethical approval

The study was approved by the Local Animal Ethical Committee (08.03.2019, no. 2019/15). Dog owners were informed about the study and signed an agreement to allow the participation of their dogs in the study.

Case description and tissue sampling

A tentative diagnosis of mammary gland tumor was made, and a mastectomy procedure was performed on the bitches admitted to the clinic (Department of Obstetrics and Gynecology, Faculty of Veterinary Medicine, Istanbul University-Cerrahpaşa) with palpable masses in mammary glands. Tissue samples were taken from the surgically removed masses. The tissues submitted for histopathological examination were fixed in 10% neutral buffered formalin. Then, the tissue was transferred to a DMEM medium (Gibco, Thermo Fisher Scientific, USA) for primary cell culture. After staining with hematoxylin and eosin, the sections were observed under a light microscope and evaluated based on the criteria defined by Goldschmidt et al. [4]. Then, three dogs diagnosed with sarcoma according to histopathological evaluation were included in the study.

Accordingly, case 1 (S1 cells) was a 22-year-old intact French Bulldog bitch, weighing 16 kg with an 8-month history of mammary mass (> 5 cm) and was diagnosed as liposarcoma. Case 2 (S2 cells) was a 12-year-old intact Cocker Spaniel bitch, weighing 15 kg with a 3-week history of mammary mass (> 10 cm) and was diagnosed as

chondrosarcoma. Case 3 (S3 cells) was a 15-year-old intact Cocker Spaniel bitch, weighing 16 kg with a 1-year history of mammary mass (> 5 cm) and was diagnosed as osteosarcoma.

Characterization of CMST cells by immunophenotyping

To visualize the expression of specific markers, the cells were cultured on a coverslip and fixed with 4% paraformaldehyde blocked in goat serum. Cells were incubated with primary antibodies of CD44 (sc-18,849, Santa Cruz Biotechnology, CA, USA), epidermal growth factor receptor (EGFR, MA5-12,875, Thermo, USA), and estrogen receptor-alpha (ER-α, ab137489, Abcam, Cambridge, UK) for 3 h at room temperature. After incubation with primary antibodies, the cells were washed and incubated for 1 h at room temperature with secondary antibodies: Goat Anti-Mouse IgG H&L (AlexaFluor® 488) (ab150117, 1:1000, Abcam, Cambridge, UK) and Goat Anti-Rabbit IgG H&L (Alexa Fluor® 488) (ab150081, 1:1000, Abcam, Cambridge, UK). Afterward, the nuclei of cells were stained with 4′,6-diamidino-2-phenylindole (DAPI, Sigma, USA) dye. Finally, images were analyzed with the EVOS Floid Cell Imaging Station (Thermo Fisher Scientific, USA).

Cell culture and PDT conditions

CMSTs that were used in this study were described in the case description and diagnosed liposarcoma, chondrosarcoma and osteosarcoma. Primary cell isolation and culture from CMST tissues were conducted as described by Turna et al. [17]. Additionally, the procedure of 5-ALA incubation and PDT treatment and protoporphyrin IX (PpIX) accumulation was conducted according to our previous studies [17, 18].

Experiments were done with a previously developed laser system [19]. The peak wavelength of the PDT laser was 635. The whole system width half maximum (FHWM) was 3 nm. The PDT system consists of four different radiation modes. The energy density of CW and PR was 9 J/cm^2. The optical output of the radiation modes was 30 mW/cm^2. The PR period was 500 ms. The CW and PR mode times were 300 and 600 s, respectively. The system was verified with (PM100 and C series spectrometer, Thorlabs, Germany). The laser system was calibrated according to the fiber optic output with optic power feedback. The PDT laser system irritation was uniform due to fiber optic cable specification [19]. The corner of the well plates was used to prevent scattering light radiation from affecting the other wells. Each well plate was prepared at a different time to use one well at a time to prevent any extended waiting period problem.

Additionally, three different experiments were conducted at different times to validate the experiment's success.

Cell viability assay

Previously, we determined the most effective PDT procedure for liposarcoma CMST cells [17], and thus, we used the most effective PDT treatment procedure in three different histological types of sarcoma (S) cells. For this purpose, an equal number of the cells (2×10^4 well/cell) were seeded in the 96-well plates and incubated for 24 h. After incubation, the S1, S2, and S3 cells were incubated with 1 mM 5-ALA in DMEM medium (Gibco, Thermo Fisher Scientific, USA) without fetal bovine serum (FBS, Gibco, Thermo Fisher Scientific, USA) for 4 h in a humidified incubator. At the end of the incubation, cell culture media was changed with a fresh medium supplemented by FBS, and the cells were irradiated with 9 J/cm^2 in CW and PR mode [17]. After irradiation, the cells were further incubated for 24 h and WST-1 dye (BioVision, San Francisco, CA, USA) was added to each well. Following incubation for 45 min at 37 °C in a humidified incubator (Thermo Fisher Scientific, USA), the absorbance values of wells was determined through the microplate reader (Allsheng, China) at 450 nm.

Reactive oxygen species (ROS) analysis

To evaluate the effect of PDT treatment on intracellular ROS levels in CMST cells (S1, S2, and S3), we conducted DCFDA/H2DCFDA Cellular ROS Assay Kit (ab113851). For this purpose, an equal number of the cells (2×10^4 well/cell) were seeded in the 96-well plates and incubated for 24 h. After incubation, the cells were incubated with 1 mM 5-ALA in DMEM medium without FBS for 4 h in a humidified incubator. At the end of the incubation, cell culture media was changed with a fresh medium supplemented by FBS, and the cells were irradiated with 9 J/cm^2 in CW and PR mode. After irradiation, the DCFDA solution was added to each well and incubated at 37 °C in the dark. After incubation for 3 h, the intracellular ROS level was analyzed in the microplate reader (Allsheng, China) at Ex/Em = 485/535 nm.

Annexin V assay

To determine the apoptotic effect of 5-ALA/PDT treatment on CMST cells (S1, S2, and S3), we conducted Annexin V & Dead Cell Assay kit (Luminex Corporation, Austin, Texas, USA). For this purpose, an equal number of the cells (1×10^5 well/cell) were seeded in the 12-well plates and incubated for 24 h. After incubation, the cells were incubated with 1 mM 5-ALA and irradiated with 9 J/cm^2 in CW and PR mode. After irradiation and incubation for 24 h, the cells

were collected and washed in phosphate buffer saline (PBS, Thermo Fisher Scientific, USA) three times and centrifuged at 1500 rpm 5 min. The cell pellet was stained with Annexin V & Dead Cell Assay kit and incubated for 30 min. Stained cells were analyzed using Muse Cell Analyzer (Millipore, Germany).

Acridine orange/propidium iodide (AO/PI) dual staining

To further analyze the apoptotic effect of PDT treatment on CMST cells (S1, S2 and S3), we stained cells with AO/PI. For this purpose, an equal number of the cells (5×10^5 well/cell) were seeded in the 6-well plates and incubated for 24 h. After incubation, the cells were incubated with 1 mM 5-ALA and irradiated with 9 J/cm^2 in CW and PR mode. After irradiation and incubation for 24 h, the cells were fixed with 4% paraformaldehyde and washed with PBS three times. After staining with AO/PI (Sigma, USA) for 30 min in the dark, the cells were visualized with the EVOS FL Cell Imaging System (Thermo Fisher Scientific, USA).

Real-time polymerase chain reaction (RT-PCR) analysis

An equal number of the cells (1×10^6 well/cell) were seeded in the 6-well plates and incubated for 24 h. After incubation, the cells were incubated with 1 mM 5-ALA and irradiated with 9 J/cm^2 in CW and PR mode. Then, total RNA was extracted with Total RNA Kit (Omega Bio-Tek) according to the manufacturer's instructions and the concentrations of isolated total RNA were determined with Qubit 4 Fluorometer (Thermo Fisher Scientific, USA). Afterward, cDNA was synthesized from isolated total RNA with High Capacity cDNA Reverse Transcription Kit (Thermo Fisher Scientific, USA). *Bax* (Cf02727746_g1), *Bcl-2* (Cf02741602_m1), *PARP1* (Cf02630973_m1), *Caspase-3* (Cf02622236_m1), and *Caspase-9* (Cf02627331_m1) mRNA expression levels were determined by TaqMan PCR Master Mix (Thermo Fisher Scientific, USA) in Step One Plus TM Real-Time PCR (Applied Biosystems, USA), and *beta-actin* (Cf04931159_m1) was used as an internal control gene.

Western Blot

To further evaluate the effect of PDT treatment on Bax, Bcl-2, PARP1, Caspase-3, and Caspase-9 protein levels, we performed the Western Blot assay. For this purpose, an equal number of the cells (1×10^6 well/cell) were seeded in the 6-well plates and incubated for 24 h. After incubation, the cells were incubated with 1 mM 5-ALA and irradiated with 9 J/cm^2 in CW and PR mode. After irradiation and incubation for 24 h, the total protein was extracted with RIPA

lysis buffer (Santa Cruz Biotechnology, CA, USA), and the total protein concentration was measured by a Qubit 4 Fluorometer (Thermo Fisher Scientific, USA). Isolated proteins were separated with 4–15% Mini-PROTEAN® TGX Stain-Free™ Protein Gels (Bio-Rad, San Diego, CA, USA) and transferred to the nitrocellulose membranes (Bio-Rad, San Diego, CA, USA). The membranes were blocked in 5% non-fat milk in tris-buffered saline with 0.1% Tween 20 (TBS-T, Bio-Rad, San Diego, CA, USA). Afterward, the membranes were incubated with appropriate primary antibodies [Anti-Bax (NB100–56,096), Anti-Bcl-2 (NB100–56,098), Anti-Caspase-9 (NB100–56,118), Anti-Caspase-3 (NB600-1235), Anti-PARP1 (436,400, Thermo), and Anti-β-Actin (sc-47,778) (Santa Cruz Biotechnology, CA, USA)] during overnight. Finally, the membranes were incubated with goat anti-mouse and rabbit immunoglobulin G (IgG) H&L (HRP; ab6789, ab6741, Abcam, Cambridge, UK) secondary antibodies for 1 h, and chemiluminescent bands were visualized by ECL detection kit (Biovision, San Francisco, CA, USA) with a G-box imaging system (Syngene).

Statistical analysis

The statistical analysis was performed by SPSS 22.0 and presented as the mean $\pm$ standard deviation of three independent experiments. For multiple comparisons, one-way analysis of variance (ANOVA) followed by Tukey's test was used, and p values less than 0.05 were considered statistically significant. To evaluate the mRNA expression analysis results, $2^{-\Delta\Delta CT}$ method was used and normalized to β-actin.

Results

Histopathological evaluation

The first case diagnosed as well-differentiated liposarcoma revealed high cellular, mature adipocytic cells and neoplastic lipoblasts with nuclear pleomorphism, prominent nucleoli, and vacuolated cytoplasm. Mitotic figures were rare (Fig. 1A–B).

Chondrosarcoma was detected as an uncommon mammary neoplasm, often multilobulated in the second case. The neoplastic cells at the periphery of the lobules were small with round hyperchromatic nuclei and occasional binucleate or multinucleate neoplastic cells. The basophilic chondroid matrix associated with the neoplastic nuclei was variable in amount (Fig. 1C–D).

The third case was diagnosed as osteoblastic osteosarcoma. There was a proliferation of cells within the neoplasm that vary from fusiform to stellate to ovoid,

Fig. 1 Histological analysis of CMST. **A–B** A wide area consisted of lipoblasts and well-differentiated lipocytes. **C–D** Atypical chondroblastic cells arranged as round foci (star), original mammary alveoli (arrow). **E** Osteoid material among osteoblastic cells (orange arrow), original mammary alveoli (black arrow). **F** A mitotic figure (orange arrow) and multinucleated osteoblastic cells scattered among neoplastic osteoblast (black arrow), H&E staining, scale = 20 μm
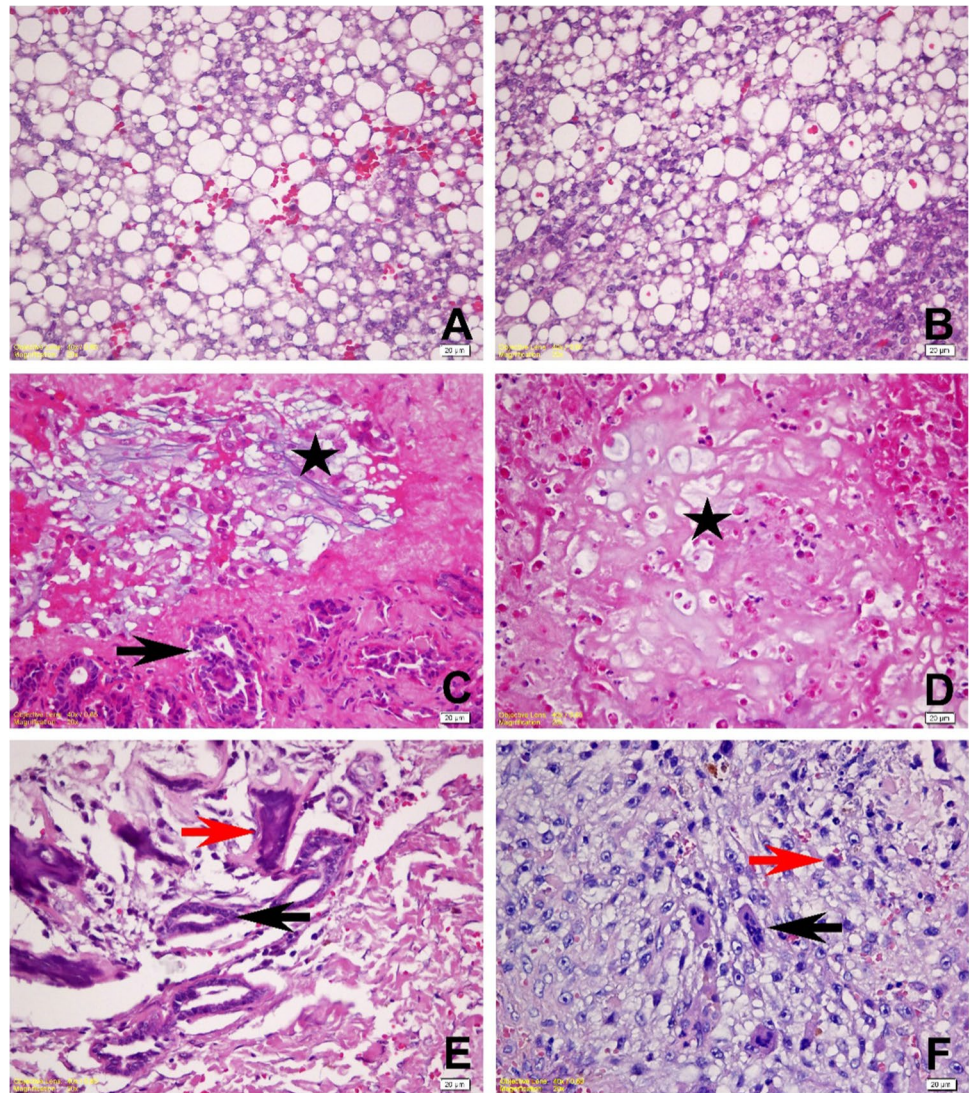
as associated with small islands of tumor osteoid and/or bone formation. Osteoblastic cells were highly atypical, and nuclei were large and clear; nucleoli were prominent. There were multinucleated osteoblastic cells in certain areas. Mitoses were frequently found (Fig. 1E–F).

Characterization results of CMST cells

The immunofluorescence method was performed to characterize CMST cells, and the expression of CD44, EGFR, and ER-α proteins was visualized in all CMST cells, as shown in Fig. 2. Our findings showed EGFR, ER-α, and CD44 cytoplasmic expression in the S1, S2, and S3 cells. However, higher cytoplasmic expression of EGFR, ER-α, and CD44 was observed in S3 cells than S1 and S2 cells. Additionally, the nuclear ER-α expression did not detect in CMST cells.

The effect of 5-ALA/PDT treatment on the viability and ROS level of CMST cells

To evaluate the inhibitory effects of 5-ALA/PDT treatment on the cell viability of CMST cells after irradiation, we performed WST-1 analysis (Fig. 3). After irradiation, the S1, S2, and S3 viability were significantly decreased compared to the control group ($p < 0.01$) (Fig. 3A). Following irradiation of S1, S2, and S3 cells in CW mode, the viability was $63.5 \pm 1.02\%$, $69.7 \pm 2.2\%$, and $58.9 \pm 0.6\%$, respectively. Furthermore, a significant decrease ($50.7 \pm 0.50\%$) was found after irradiation in PR mode in S2 cells compared with the control group ($p < 0.01$) (Fig. 3A). In this context, a significant difference between the suppression of the cell viability of S1, S2, and S3 cells was determined in terms of CW and PR modes (Fig. 3C). We further evaluated the intracellular ROS level after irradiation with the energy density of 9 J/cm^2 in two different modes. Our findings demonstrated
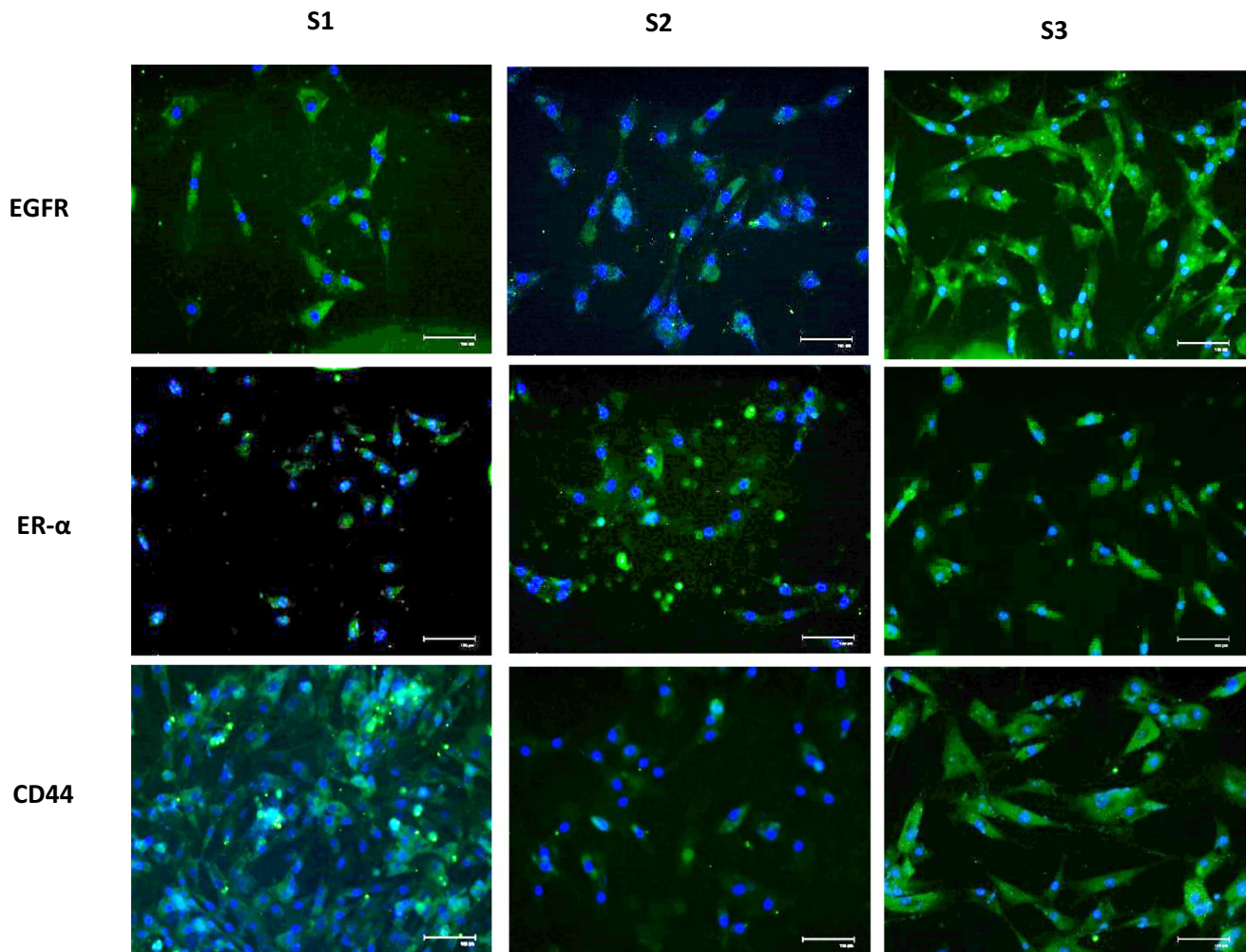
Fig. 2 The expression of CD44, EGFR and ER-α proteins was observed in all CMGS cells through immunofluorescence staining (scale = 100 μm)

that 5-ALA PDT significantly increased the ROS level in both two different modes in all CMST cells compared to the control group ($p < 0.01$) (Fig. 3B). However, a significant increase in the ROS level was found in S1 and S2 cells in PR mode compared with the control group ($p < 0.01$) (Fig. 3B). However, there was no significant difference between the intracellular ROS level and CW and PR modes in S1, S2, and S3 cells (Fig. 3D). Therefore, we concluded that 5-ALA-based PDT significantly suppressed the viability of CMST cells and caused a significant increase in the intracellular ROS level in both radiation modes.

The effect of PDT treatment on apoptotic cell death in CMST cells

We performed Annexin V analysis to evaluate the apoptotic effects of PDT treatment on CMST cells (Fig. 4). After irradiation with CW and PR modes, the rate of apoptotic cells was significantly increased in all CMST cells compared to the control group ($p < 0.01$) (Fig. 4A). The percentage of total apoptotic S1 cells considerably increased from $1.7 \pm 0.4\%$ to $41.8 \pm 0.4\%$ and $33.2 \pm 0.6\%$ in CW and PR modes, respectively ($p < 0.01$). Similarly, the total apoptotic cell rate increased from $3.5 \pm 0.4\%$ to $25.4 \pm 0.7\%$ and $36.1 \pm 0.4\%$ in S3 cells in both CW and PR modes, respectively, compared with the control group ($p < 0.01$, Fig. 4B). On the other hand, a significant increase ($56.9 \pm 0.6\%$) in the total percentage of apoptotic S2 cells was detected in PR mode compared with the control group ($p < 0.01$, Fig. 4B). Additionally, there was a significant difference between the percentage of apoptotic cells and CW and PR modes in S1, S2, and S3 cells ($p < 0.01$, Fig. 4C). Therefore, 5-ALA-based PDT treatment induced apoptotic cell death in all CMST cells. However, 5-ALA-mediated apoptotic effects differed in CMST cells upon CW and PR irradiation. S2 cells were more sensitive to 5-ALA/PDT after irradiation with PR
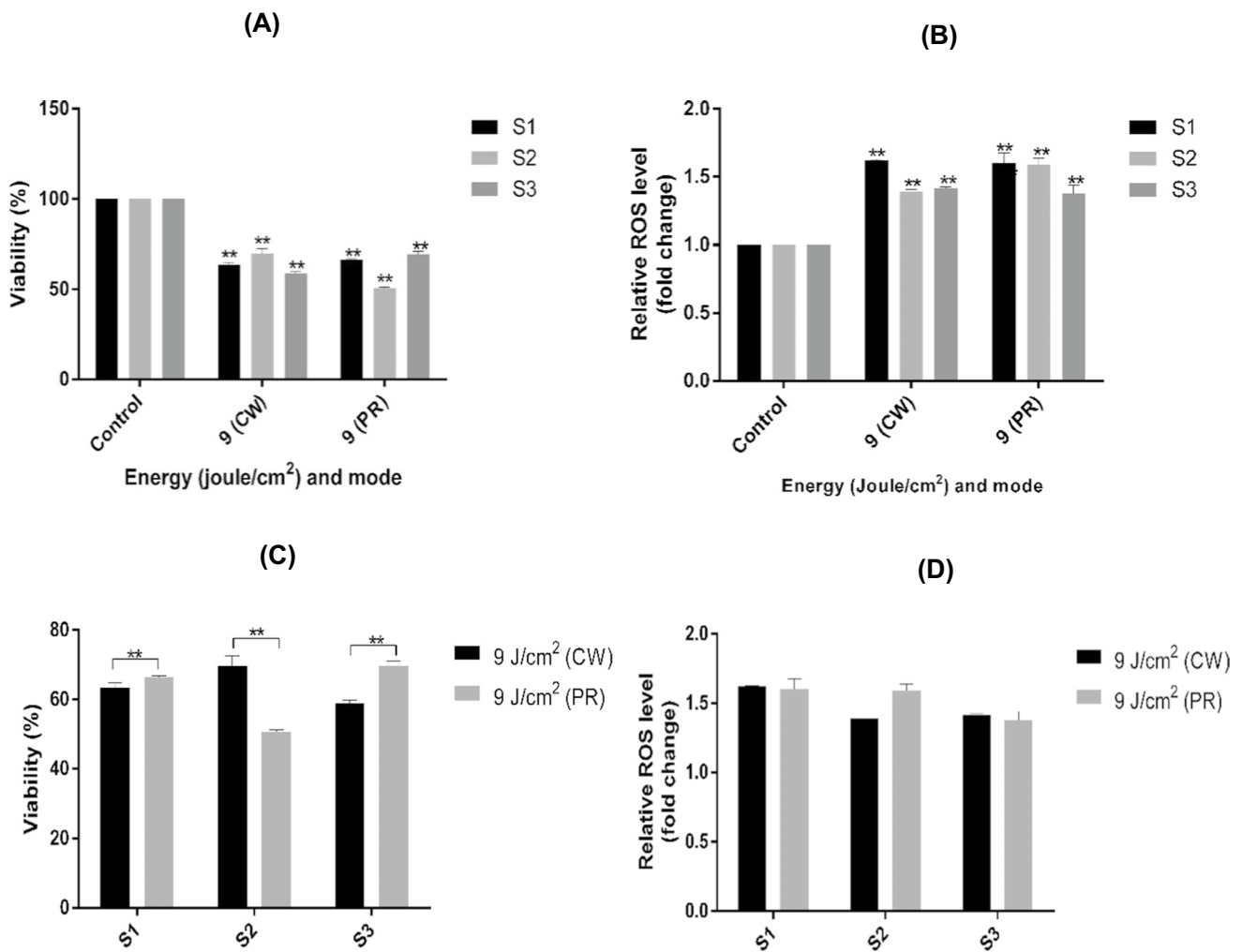
(A)

(B)

(C)

(D)

Fig. 3 The effect of PDT treatment on the cell viability and ROS level in CMST cells. **A** The result of WST-1 analysis and **B** the results of intracellular ROS level. The statistical comparison of CW with PR in **C** the cell viability and **D** relative ROS level (CW, continuous wave; PR, pulse radiation, $p < 0.01$**)

mode than S1 and S3 cells, whereas 5-ALA-induced apoptosis was more profound in S1 cells in CW mode.

The effect of PDT treatment on the morphological changes of CMST cells

To further evaluate the apoptotic effects of 5-ALA/PDT treatment on CMST cells, we observed the morphological changes of cells by AO/PI staining (Fig. 5). We observed cell shrinkage and especially nuclear blebbing in all CMST cells following irradiation with CW and PR modes compared with control cells (Fig. 5). Therefore, 5-ALA treatment especially caused early apoptosis in CMST cells, and our results were consistent with the Annexin V analysis results. However, 5-ALA induced more nuclear damage in S2 cells than S1 and S3 cells.

The effect of PDT treatment on the alteration of gene and protein expression in CMST cells

To determine the expression of Bax, Bcl-2, PARP, Caspase-3, and Caspase-9 mRNA and protein levels after 5-ALA/PDT treatment, we conducted RT-PCR and Western blot analysis (Fig. 6). *Bax* mRNA level significantly upregulated in S2 and S3 cells after irradiation with CW (1.4-, 1.4-, and 1.3-fold, respectively) and PR (1.5-, 1.7-, and 1.5-fold, respectively) modes ($p < 0.01$) with the downregulation of *Bcl-2* mRNA levels (Fig. 6A). Additionally, higher upregulation of *Caspase-3 and Caspase-9* mRNA levels was observed in S1, S2, and S3 cells upon irradiation by CW (S1: 3.4- and 3.2-fold, S2: 4.0- and 3.9-fold, S3: 3.7- and 3.6-fold, respectively) and PR (S1: 5.5- and 6.1-fold, S2: 7.6- and 7.6-fold, S3: 5.9- and 7.2-fold, respectively) modes ($p < 0.01$) (Fig. 6A). Furthermore,
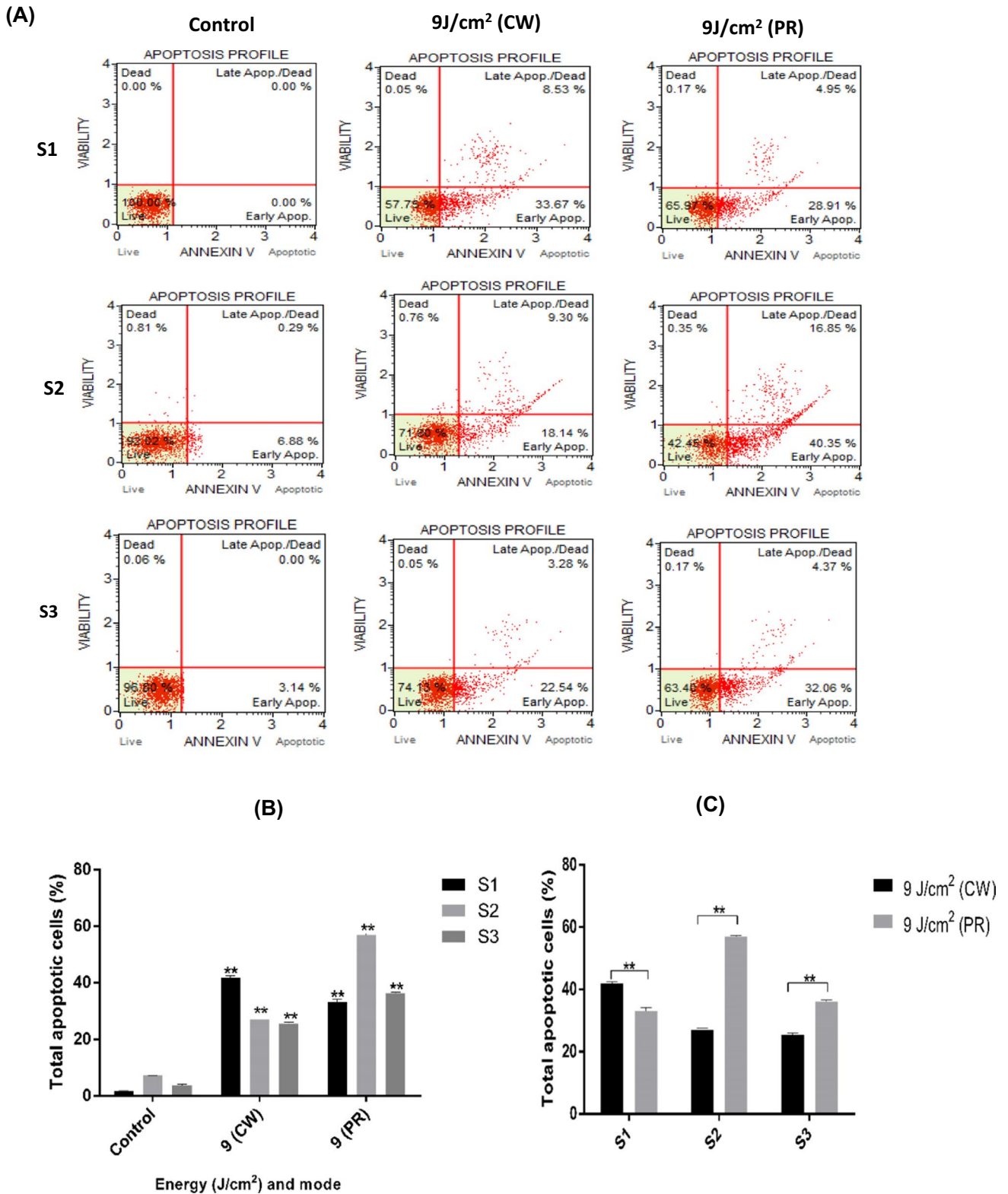
(A)

(B)   **(C)**

Fig. 4 The effect of PDT treatment on apoptotic cell death rate of CMST cells. **A** The percentage of apoptotic cells was analyzed by Annexin V analysis. Statistical comparison of **B** the total apoptotic S1, S2, and S3 cells and **C** CW and PR mode (CW, continuous wave; PR, pulse radiation, $p < 0.01$**)
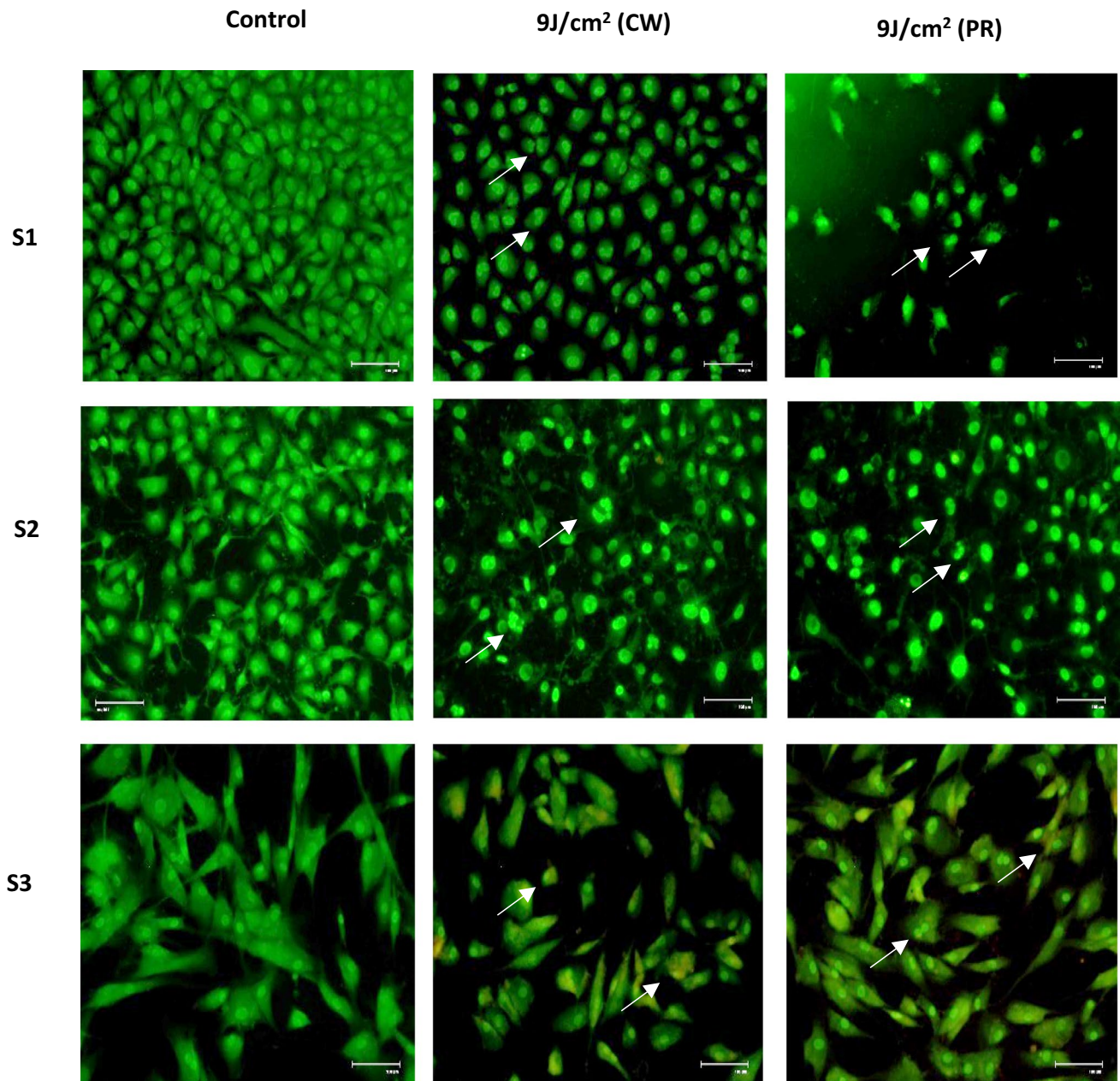
Fig. 5 The effect of PDT treatment on the morphological changes of CMST cells was observed by AO/PI dual staining (CW, continuous wave; PR, pulse radiation)

cleaved Caspase-3 and Caspase-9 protein expression was upregulated in S1 cells after irradiation by CW and PR modes. However, we did not observe protein levels of Bax, Bcl-2, and cleaved Caspase-3 and Caspase-9 in S3 cells following 5-ALA/PDT treatment despite increased total Caspase-3 and Caspase-9 protein levels. Additionally, the over-expression of PARP1, cleaved Caspase-9, and Caspase-3 proteins was detected in S2 cells, and thus PR mode was more effective than CW mode in S2 cells at both mRNA and protein levels (Fig. 6B).

Discussion

Herein, we, for the first time, revealed that 5-ALA-based PDT exerted potential therapeutic effects on CMST cells. Our results showed that S2 chondrosarcoma cells were more responded to 5-ALA/PDT in PR mode than CW mode. Additionally, the anti-cancer activity of 5-ALA was more profound in S1 liposarcoma cells than in S3 osteosarcoma cells in CW modes. Therefore, the response of three different histological types of CMST cells to 5-ALA/PDT was
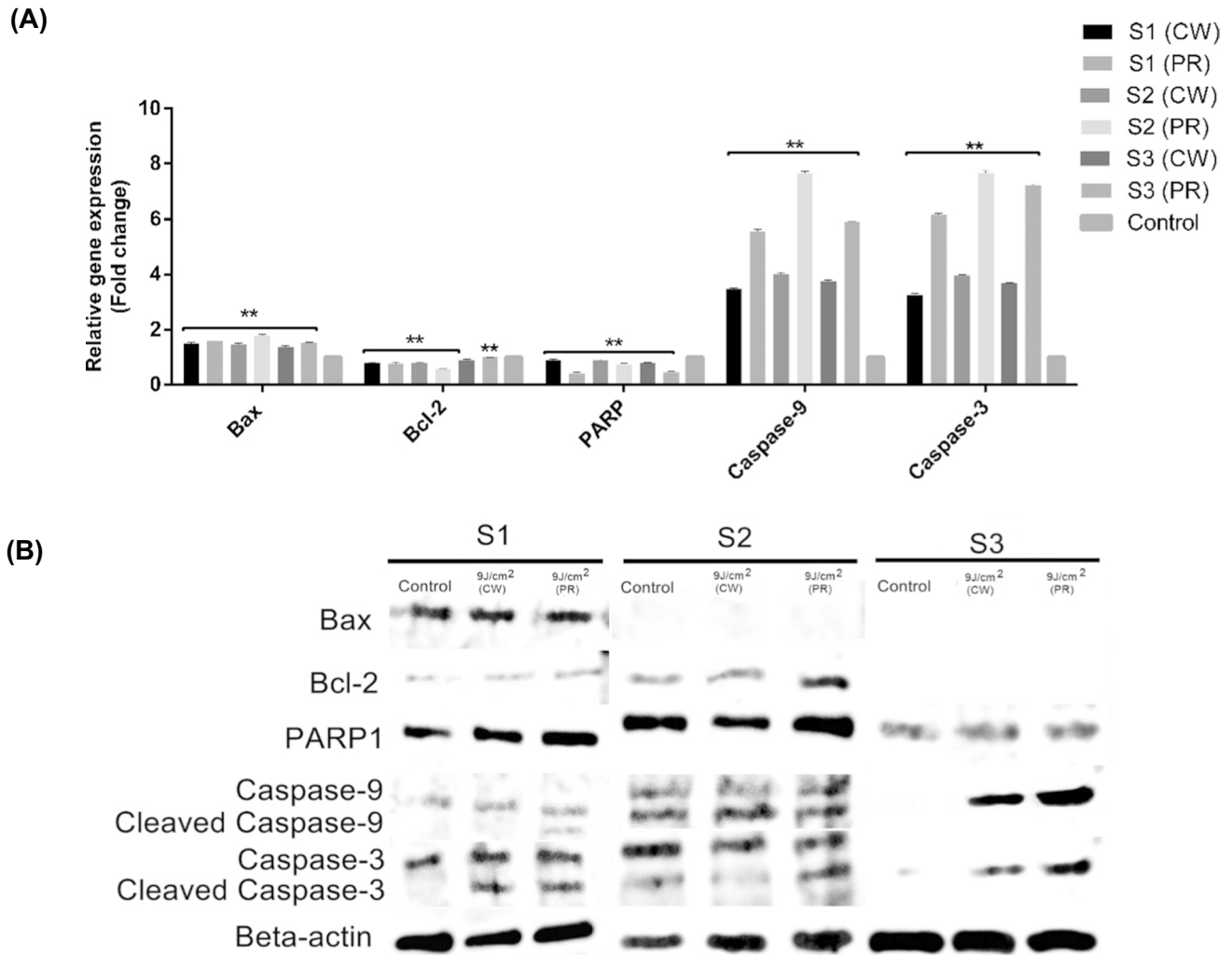
(A)

(B)

Fig. 6 The effect of PDT treatment on the alteration of gene and protein expressions in CMST cells. **A** The changes in mRNA level of *Bax*, *Bcl-2*, *PARP1*, *Caspase-3*, and *Caspase-9* genes were deter-mined by RT-PCR analysis and **B** the protein level of Bax, Bcl-2, PARP1, Caspase-3, and Caspase-9 was analyzed by Western Blot analysis (CW, continuous wave; PR, pulse radiation)

different due to their characteristic features. Additionally, 5-ALA induced apoptosis via externalizing phosphatidyl-serine, increased ROS level, and upregulated Bax and Cas-pase-9 and Caspase-3 mRNA and protein levels, especially S1 and S2 cells.

CMSTs are a very rare tumor type with a poor prognosis, higher levels of Ki-67 and consisting of heterogeneous groups [20]. Furthermore, the expression of ERα or pro-gesterone receptors is not detected in CMST; thus, hormonal therapy is not beneficial for treating CMST [21]. In this context, we did not observe any nuclear ER-α expression in all CMST cells. However, higher cytoplasmic expression levels of EGFR and CD44 were observed due to the aggressiveness of CMST. Many CMGT exert ER expression. However, some of them do not respond to hormone therapy due to possibly ERα localization [20, 21]. In Li et al. [22] study, ERα66 is mainly expressed in the nucleus, whereas

ERα36 is localized in the cytoplasm and/or membrane in human breast cancer. Additionally, cytoplasmic ERα expression promotes survival in mouse mammary cancer cell lines [23]. On the other hand, there is no correlation between the absence of ERα and the proliferation status of CMST [20]. Therefore, further validation studies, such as flow cytometry analysis, are required to elucidate the underlying molecular mechanisms of ERα and the association of cellular ER localization with its activity in CMST.

Recent studies have focused on the effectiveness of PDT or photodynamic detection (PDD) through various photosensitizers for CMT treatment [15–17, 24–28]. However, there is no study evaluating the efficacy of 5-ALA-based PDT in treating different histological types of CMST alone. Our preliminary findings showed that 5-ALA/PDT could potentially inhibit the proliferation of CMST cells and its cytotoxicity was more profound in especially S2

chondrosarcoma cells than in S1 liposarcoma cells and S3 osteosarcoma cells. Furthermore, the anti-cancer activity of 5-ALA/PDT could result from apoptotic cell death via increased intracellular ROS level and overexpression of Bax and Caspase-9 and Caspase-3 mRNA and protein levels in CMST cells, particularly S1 and S2 cells. In the literature, HMME-based PDT causes apoptotic cell death in CMT cells through the up-regulation of Caspase-9, Caspase-3, and Bax levels [26, 27]. Additionally, the molecular mechanisms of 5-ALA-mediated apoptosis have been revealed in different types of human cancer cell lines [29–32]. In this context, we first provided evidence that 5-ALA treatment resulted in especially early apoptosis in different groups of CMST following irradiation with different modes. However, further studies need to assess the efficacy of 5-ALA in other histological types (fibrosarcoma and hemangiosarcoma) of CMST and its molecular mechanisms in each group of CMST.

Furthermore, 5-ALA/PDT was more effective in especially S2 cells after irradiation with 9 J/cm^2 by PR mode. On the other hand, S1 cells were more sensitive to 5-ALA/PDT after irradiation by CW mode at 9 J/cm^2. In PDT treatment, increased cytotoxicity is related to higher cumulative $^1O_2$ concentration with decreased consumption of photochemical triplet oxygen ($^3O_2$). CW irradiation provides intensive $^3O_2$ depletion with a high fluence rate and thus induces less cytotoxicity and necrosis. However, the inter-pulse interval in PR irradiation where no light is incident on the cells corresponds to 50% of the overall irradiation time. Thus, PR mode could reduce oxygen depletion, enhance the singlet oxygen generation, induce apoptosis, and avoid hypoxia [33, 34]. In the study of Klimenko et al. [33], 3 μM Radachlorin causes apoptotic cell death in k562 cells after PR irradiation at 1–5 J/cm^2, unlike CW irradiation. Additionally, the cells exposed to the pulsed light consume a lower amount of oxygen compared with CW mode due to the prevention of cell stress from temperature changes [34]. Therefore, oxygenation status could potentially affect PDT efficiency. Therefore, the different responses of CMST cells to 5-ALA/PDT upon CW and PR irradiation at 9 J/cm^2 could result from depletion or preservation of oxygenation during PDT treatment. Furthermore, combination of PDT and PTT based on nanoparticles is a new treatment strategy for cancer to provide efficient targeting of cancer cells using photosensitive and photothermal agents [35]. Asrar et al. (2022) state that photothermal therapy (PTT) of melanoma cells through carbon nanotubes is selectively killed and induces necrosis due to their weakened heat resistance compared with normal tissue [36]. Additionally, PEGylated carbon nanotubes decorated with silver nanoparticles destroy malignant melanoma tumors through the PTT via a continuous wave NIR laser

diode ($\lambda = 808$ nm, P $= 2$ W, and I $= 2$ W/cm^2) [37]. Therefore, further studies will be performed for the identification of novel combined PDT and PTT treatment modalities for CMST cells.

Finally, the mRNA levels of *Bcl-2* and *PARP1* were decreased in all CMST cells after irradiation in both modes. However, the protein expression levels of Bcl-2 and PARP1 were upregulated in S1 and S2 cells. A lack of correlation between reduced mRNA level and abundance in protein level may result from uncontrolled or tightly controlled mRNA expression, half-lives of protein synthesis, and post-transcriptional or translational modifications [38, 39]. Therefore, the molecular mechanism of these differences between mRNA and protein levels needs further investigation.

Herein, we assessed the therapeutic potential of 5-ALA-based PDT in three different CMST cells for the first time. Our preliminary findings showed that 5-ALA potentially inhibited the growth of CMST cells and caused apoptotic cell death. Therefore, 5-ALA/PDT could be a promising alternative treatment strategy for the treatment of CMST. However, the response of three different CMST cells to 5-ALA/PDT was different upon CW and PR modes at the same fluence rate. Thus, the therapeutic potential of 5-ALA/PDT will be further investigated in both canine and human breast cancer at the molecular level to determine the most effective PDT treatment in vitro and in vivo studies. Furthermore, the combination of 5-ALA/PDT and PTT studies will be performed to obtain higher therapeutic efficiency for the treatment CMST.

Declarations

Ethical approval The study was approved by the Local Animal Ethical Committee (08.03.2019, no. 2019/15).

Competing interest The authors declare no competing interests.

References

1. Sorenmo K (1998) An update on canine mammary gland tumors. ACVIM Forum 16:387–388
2. Sorenmo K (2003) Canine mammary gland tumors. Vet Clin North Am Small Anim Pr 33:573–596
3. Beveridge WI, Sobin LH (1976) International histological classification of tumours of domestic animals: introduction. Bull World Health Organ 50(1–2):1–6
4. Goldschmidt MH, Peña L, Rasotto R, Zappulli V (2011) Classification and grading of canine mammary tumors. Vet Pathol 48:117–131. https://doi.org/10.1177/0300985810393258
5. Von Euler H (2011) Tumours of the mammary glands. In: LD Dobson JM (ed), Canine feline oncology, 3rd edn. BSAVA, Gloucester, pp 237–247. https://doi.org/10.22233/9781905319749.16
6. Liptak F, Forrest JM (2017) Mesenchymal tumors of the skin and soft tissues. In: Meuten D (ed) Tumors domestic animals, 4th edn. Iowa State Press, Ames, pp 142–175
7. Hendrick MJ (2017) Mesenchymal tumors of the skin and soft tissues. In: Meuten DJ (ed) Tumors domestic animals, 4th edn. Iowa State Press, pp 142–175. https://doi.org/10.1002/9781119181200.ch5
8. McKnight JA, Mauldin GN, McEntee MC, Meleo KA, Patnaik AK (2000) Radiation treatment for incompletely resected soft-tissue sarcomas in dogs. J Am Vet Med Assoc 217:205–210. https://doi.org/10.2460/javma.2000.217.205
9. Gentschev I, Adelfinger M, Josupeit R, Rudolph S, Ehrig K, Donat U, Weibel S, Chen NG, Yu YA, Zhang Q, Heisig M, Thamm D, Stritzker J, Macneill A, Szalay AA (2012) Preclinical evaluation of oncolytic vaccinia virus for therapy of canine soft tissue sarcoma. Plos One 7:1–12. https://doi.org/10.1371/journal.pone.0037239
10. Banerjee SM, MacRobert AJ, Mosse CA, Periera B, Bown SG, Keshtgar MRS (2017) Photodynamic therapy: inception to application in breast cancer. Breast 31:105–113. https://doi.org/10.1016/j.breast.2016.09.016
11. Kwiatkowski S, Knap B, Przystupski D, Saczko J, Kędzierska E, Knap-Czop K, Kotlińska J, Michel O, Kotowski K, Kulbacka J (2018) Photodynamic therapy – mechanisms, photosensitizers and combinations. Biomed Pharmacother 106:1098–1107. https://doi.org/10.1016/j.biopha.2018.07.049
12. Hamblin MR (2020) Photodynamic therapy for cancer: what's past is prologue. Photochem Photobiol 96:506–516. https://doi.org/10.1111/php.13190
13. Nokes B, Apel M, Jones C, Brown G, Lang JE (2013) Aminolevulinic acid (ALA): photodynamic detection and potential therapeutic applications. J Surg Res 181:262–271. https://doi.org/10.1016/j.jss.2013.02.002
14. Casas A (2020) Clinical uses of 5-aminolaevulinic acid in photodynamic treatment and photodetection of cancer: a review. Cancer Lett 490:165–173. https://doi.org/10.1016/j.canlet.2020.06.008
15. Osaki T, Yokoe I, Sunden Y, Ota U, Ichikawa T, Imazato H, Ishii T, Takahashi K, Ishizuka M, Tanaka T, Li L, Yamashita M, Murahata Y, Tsuka T, Azuma K, Ito N, Imagawa T, Okamoto Y (2019) Efficacy of 5-aminolevulinic acid in photodynamic detection and photodynamic therapy in veterinary medicine. Cancers (Basel) 11, 95. https://doi.org/10.3390/cancers11040495
16. Ridgway TD, Lucroy MD (2003) Phototoxic effects of 635-nm light on canine transitional cell carcinoma cells incubated with 5-aminolevulinic acid. Am J Vet Res 64:131–136. https://doi.org/10.2460/ajvr.2003.64.131
17. Turna O, Baykal A, Sozen Kucukkara E, Ozten O, Deveci Ozkan A, Guney Eskiler G, Kamanli AF, Bilir C, Yildiz SZ, Kaleli S, Ucmak M, Kasikci G, Lim HS (2021) Efficacy of 5-aminolevulinic acid-based photodynamic therapy in different subtypes of canine mammary gland cancer cells. Lasers Med Sci. https://doi.org/10.1007/s10103-021-03324-y
18. Guney Eskiler G, Deveci Ozkan A, Sozen Kucukkara E, Kamanlı AF, Gunoğlu B, Yıldız MZ (2020) Optimization of 5-aminolevulinic acid-based photodynamic therapy protocol for breast cancer cells. Photodiagnosis Photodyn Ther 31:1–7. https://doi.org/10.1016/j.pdpdt.2020.101854
19. Kamanli AF, Yildiz MZ, Arslan H, Çetinel G, Lim NK, Lim HS (2020) Development of a new multi-mode NIR laser system for photodynamic therapy. Opt Laser Technol 128:106229. https://doi.org/10.1016/j.optlastec.2020.106229
20. Dolka I, Sapierzyński R, Król M (2013) Retrospective study and immunohistochemical analysis of canine mammary sarcomas. BMC Vet Res 9:248. https://doi.org/10.1186/1746-6148-9-248
21. Yoon CS, Kang SS (2017) Primary osteosarcoma of the breast: a case report. Ann Surg Treat Res 93:57–60. https://doi.org/10.4174/astr.2017.93.1.57
22. Li L, Wang Q, Lv X, Sha L, Qin H, Wang L, Li L (2015) Expression and localization of estrogen receptor in human breast cancer and its clinical significance. Cell Biochem Biophys 71:63–68. https://doi.org/10.1007/s12013-014-0163-6
23. Smart E, Alejo LH, Frasor J (2020) Cytoplasmic ERα and NFκB promote cell survival in mouse mammary cancer cell lines. Horm Cancer 11:76–86. https://doi.org/10.1007/s12672-020-00378-2
24. Osaki T, Yokoe I, Ogura S, Takahashi K, Murakami K, Inoue K, Ishizuka M, Tanaka T, Li L, Sugiyama A, Azuma K, Murahata Y, Tsuka T, Ito N, Imagawa T, Okamoto Y (2017) Photodynamic detection of canine mammary gland tumours after oral administration of 5-aminolevulinic acid. Vet Comp Oncol 15:731–739. https://doi.org/10.1111/vco.12213
25. Burch S, London C, Seguin B, Rodriguez C, Wilson BC, Bisland SK (2009) Treatment of canine osseous tumors with photodynamic therapy: a pilot study. Clin Orthop Relat Res 467:1028–1034. https://doi.org/10.1007/s11999-008-0678-5
26. Liu Y, Ma XQ, Jin P, Li HT, Zhang RR, Ren XL, Wang HB, Tang D, Tian WR (2011) Apoptosis induced by hematoporphyrin monomethyl ether combined with He-Ne laser irradiation in vitro on canine breast cancer cells. Vet J 188:325–330. https://doi.org/10.1016/j.tvjl.2010.05.013
27. Li H, Tong J, Bao J, Tang D, Tian W, Liu Y (2016) Hematoporphyrin monomethyl ether combined with He-Ne laser irradiation-induced apoptosis in canine breast cancer cells through the mitochondrial pathway. J Vet Sci 17:235–242. https://doi.org/10.4142/jvs.2016.17.2.235
28. Osaki T, Hibino S, Yokoe I, Yamaguchi H, Nomoto A, Yano S, Mikata Y, Tanaka M, Kataoka H, Okamoto Y (2019) A basic study of photodynamic therapy with glucose-conjugated chlorin e6 using mammary carcinoma xenografts. Cancers (Basel) 11:1–19. https://doi.org/10.3390/cancers11050636
29. Mohammadpour H, Fekrazad R (2016) Antitumor effect of combined Dkk-3 and 5-ALA mediated photodynamic therapy in breast cancer cell's colony. Photodiagnosis Photodyn Ther 14:200–203. https://doi.org/10.1016/j.pdpdt.2016.04.001
30. Karmakar S, Banik NL, Patel SJ, Ray SK (2007) 5-Aminolevulinic acid-based photodynamic therapy suppressed survival factors and activated proteases for apoptosis in human glioblastoma U87MG cells. Neurosci Lett 415:242–247. https://doi.org/10.1016/j.neulet.2007.01.071
31. Fahmy UA, Fahmy O (2020) In vitro evaluation of cytotoxic properties of 5-aminolevulinic acid (5-ALA) on bladder cancer

cells. Photodiagnosis Photodyn Ther 30:101714. https://doi.org/10.1016/j.pdpdt.2020.101714

32. Chelakkot VS, Som J, Yoshioka E, Rice CP, Rutihinda SG, Hirasawa K (2019) Systemic MEK inhibition enhances the efficacy of 5-aminolevulinic acid-photodynamic therapy. Br J Cancer 121:758–767. https://doi.org/10.1038/s41416-019-0586-3

33. Klimenko VV, Knyazev NA, Moiseenko FV, Rusanov AA, Bogdanov AA, Dubina MV (2016) Pulse mode of laser photodynamic treatment induced cell apoptosis. Photodiagnosis Photodyn Ther 13:101–107. https://doi.org/10.1016/j.pdpdt.2016.01.003

34. Kawauchi S, Morimoto Y, Sato S, Arai T, Seguchi K, Asanuma H, Kikuchi M (2004) Differences between cytotoxicity in photodynamic therapy using a pulsed laser and a continuous wave laser: Study of oxygen consumption and photobleaching. Lasers Med Sci 18:179–183. https://doi.org/10.1007/s10103-004-0288-8

35. Hou YJ, Yang XX, Liu RQ, Zhao D, Guo CX, Zhu AC, Wen MN, Liu Z, Qu GF, Meng HX (2020) Pathological mechanism of photodynamic therapy and photothermal therapy based on nanoparticles. Int J Nanomed 15:6827–6838. https://doi.org/10.2147/IJN.S269321

36. Asrar A, Sobhani Z, Behnam MA (2022) Melanoma cancer therapy using PEGylated nanoparticles and semiconductor laser. Adv Pharm Bull 12(3):524–530. https://doi.org/10.34172/apb.2022.055

37. Behnam MA, Emami F, Sobhani Z (2021) PEGylated carbon nanotubes decorated with silver nanoparticles: fabrication, cell cytotoxicity and application in photo thermal therapy. Iranian J Pharm Res 20(1):91–104

38. Liu Y, Beyer A, Aebersold R (2016) On the dependency of cellular protein levels on mRNA abundance. Cell 165:535–550. https://doi.org/10.1016/j.cell.2016.03.014

39. Greenbaum M, Colangelo D, Williams C, Gerstein K (2003) Comparing protein abundance and mRNA expression levels on a genomic scale. Genome Biol 4:1–8. https://doi.org/10.1186/gb-2003-4-9-117